Pergamon

Int. J. Solids Structures Vol. 34, No. 5, pp. 625–638, 1997

0020-7683/96 $15.00 + .00

PII: S0020-7683(96)00037-6

INTERFACE STABILITY UNDER BIAXIAL LOADING OF BILAYERED SHEETS BETWEEN RIGID SURFACES—II. STABILITY OF PERTURBATIONS

J. L. ALCARAZ,
Departamento de Ingeniería Mecánica-Escuela Técnica Superior de Ingenieros, Alameda Urquijo, s n-48013 Bilbao.

J. M. MARTÍNEZ-ESNAOLA and J. GIL-SEVILLANO
Centro de Estudios e Investigaciones Técnicas de Guipúzcoa (CEIT) and Escuela Superior de Ingenieros Industriales (Universidad de Navarra)-P° Manuel de Lardizábal, 15-20009 San Sebastián.

(*Received* 23 *March* 1995)

Abstract The bifurcation analysis of a bilayered sheet between rigid surfaces under biaxial loading (Alcaraz *et al.*, 1997) is continued here by considering the stability analysis of the emerging undulations near the interface in the spacially periodic mode. Assuming an initial perturbation along the interface, conditions preventing the growth of this perturbation are studied. With this aim, a stability parameter is introduced. The influence on this parameter of the geometric and material variables is discussed in detail. It is also shown that stability strongly depends on the constitutive model assumed in the computations. Copyright © 1996 Elsevier Science Ltd.

1. INTRODUCTION

In a previous paper (Alcaraz *et al.*, 1997), a critical bifurcation strain was determined for the onset of interface instabilities in a bimetallic sheet between rigid surfaces subjected to biaxial plastic loading. Diffuse mode instabilities, leading to an undulating behaviour of the interface, were the main type of instabilities in the composite, in competition with the localized shear band formation.

Focussing on that periodic spatial mode, it should be guaranteed that the growth of the undulations remains below a critical level. Exceeding this level could result in refusable bimetallic products, because of an unacceptable thickness in one of the materials. For example, in the bimetallic extrusion, products with an extremely non-uniform thickness are sometimes obtained.

Several attempts were previously made in the analysis of instabilities. Dudzinski and Molinari (1991) carried out a perturbation analysis applied to a thermoviscoplastic material in biaxial loading. The growth of the instability was characterized by means of an effective instability. This concept was introduced to consider the rate of growth of the fastest mode. Apart from this study, more recently Triantafyllidis and Lehner (1993) analysed the interfacial instabilities of density-stratified two-layer systems under initial stress. The stability of perturbations was determined from the appropriate linearized equations of motion. The critical stress at which an initial stable stratification is destabilized was shown to depend on the wavelength of a perturbation.

In this paper, as a continuation of the previous one, a dynamic analysis of stability is applied to a bimaterial layer, placed between rigid surfaces and subjected to biaxial loading. The problem is tackled as a bifurcation problem, by considering the dynamic term in the equilibrium equations. An instability parameter defined in the analysis contemplates the growth of the initial interface undulations. The effects of the different geometric and material variables on this parameter are presented, as well as the influence of the constitutive model used in the calculations.

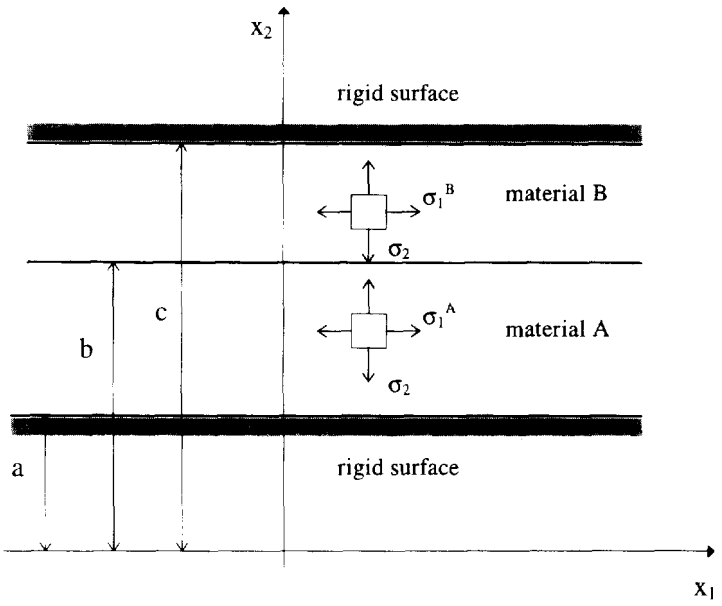

Fig. 1. Geometry of the problem.

2. FORMULATION OF THE PROBLEM

A plane bilayer with finite thickness and infinite length is subjected to biaxial loading in plane strain. Figure 1 shows the geometry of the problem: material A is placed between the planes $x_2 = a$ and $x_2 = b$, material B between $x_2 = b$ and $x_2 = c$, and the bilayer is limited by two rigid surfaces at $x_2 = a$ and $x_2 = c$.

Consider then the stability of the initially plane interface, subjected at a time instant $t = 0$ to a perturbation of small amplitude (ε) and arbitrary wavelength, around the equilibrium state.

The linearized equations of motion, in the absence of body forces, lead to the expression:

$$n_{ij,j} = \rho \ddot{u}_i \tag{1}$$

where n_{ij} represents the nominal stress tensor, $(\ )_{,i}$ meaning the partial differentiation with respect to x_i; $\ddot{u}_i$ is the acceleration vector, u_i being the displacement vector, and ρ is the density.

We can write all the quantities in the perturbed system as a sum of their corresponding fundamental (unperturbed) values, plus a term which depends on the amplitude of the initial disturbance, ε. In particular:

$$\begin{aligned} n_{ij} &= n_{ij}^{\circ} + \varepsilon \tilde{n}_{ij} + 0(\varepsilon^2) \\ u_i &= u_i^{\circ} + \varepsilon \tilde{u}_i + 0(\varepsilon^2) \end{aligned} \tag{2}$$

where n_{ij}°, u_i° are the fundamental values, and $\varepsilon \tilde{n}_{ij}$, $\varepsilon \tilde{u}_i$ are the linear terms of the perturbed magnitudes.

By inserting (2) in (1), the first order approximation yields:

$$\tilde{n}_{ij,j} = \rho \ddot{\tilde{u}}_i. \tag{3}$$

On the other hand, the continuity conditions at the bimaterial interface can be written in terms of the perturbed values:

$$\langle \tilde{n}_{ij} N_i \rangle = 0, \langle \tilde{u}_i \rangle = 0 \tag{4}$$

where the sign $\langle\ \rangle$ indicates the jump in the enclosed magnitude across the interface, and N_i are the components of the outward normal. The boundary conditions imply that the velocity component v_2 vanishes at $x_2 = a$ and $x_2 = c$.

Assuming that the hydrostatic pressure does not affect the relation between the deviators of stress rate and strain rate, the constitutive equation for incrementally-linear solids is expressed in the following form (Biot, 1965):

$$\begin{aligned} \hat{\sigma}_{11} &= \hat{\sigma}_{22} = 2\mu^*(\varepsilon_{11} - \varepsilon_{22}) \\ \hat{\sigma}_{12} &= 2\mu\varepsilon_{12} \\ \hat{\sigma}_{21} &= \hat{\sigma}_{12} \end{aligned} \tag{5}$$

where $\hat{\sigma}_{ij}$ is the Jaumann derivative (referred to the rotating axes) of the true stress, ε_{ij} is the Eulerian strain rate, $\varepsilon_{ij} = (\dot{u}_{i,j} + \dot{u}_{j,i})/2$, $\dot{u}_i$ being the velocity, μ, μ^* are two incremental shear moduli. The linearization applies similarly to (5) yielding:

$$\begin{aligned} \dot{\tilde{\sigma}}_{11} - \dot{\tilde{\sigma}}_{22} &= 2\mu^*(\dot{\tilde{u}}_{1,1} - \dot{\tilde{u}}_{2,2}) \\ \dot{\tilde{\sigma}}_{12} &= \dot{\tilde{\sigma}}_{21} = \mu(\dot{\tilde{u}}_{1,2} + \dot{\tilde{u}}_{2,1}) \end{aligned} \tag{6}$$

As the coefficients of the linearized equations do not depend on time, we can find solutions in the form:

$$\begin{aligned} \tilde{u}_i(x_1, x_2, x_3, t) &= e^{\xi^2 t} \bar{u}_i(x_1, x_2, x_3) \\ \tilde{n}_{ij}(x_1, x_2, x_3, t) &= e^{\xi^2 t} \bar{n}_{ij}(x_1, x_2, x_3). \end{aligned} \tag{7}$$

By inserting (7), (3) turns into

$$\bar{n}_{ij,j} + \rho\xi^2 \bar{u}_i = 0 \tag{8}$$

and the continuity conditions at the interface (4) can be written as

$$\langle \bar{n}_{ij} N_i \rangle = 0, \quad \langle \bar{u}_i \rangle = 0. \tag{9}$$

Note that ξ^2 is the linear eigenvalue of (8). For a constitutive law

$$\bar{n}_{ij} = L_{ijkl} \bar{u}_{l,k} \tag{10}$$

where L_{ijkl} is a tensor of incremental moduli satisfying the symmetry condition $L_{ijkl} = L_{klij}$, all the eigenvalues are proved to be real (Triantafyllidis and Lehner, 1993). When the minimum of these eigenvalues, ξ_m^2 satisfies $\xi_m^2 > 0$, solution (7) will remain bounded with time and the interface will be stable. It should be noted that no dissipation mechanism is considered here. This would produce a decaying amplitude solution. For $\xi_m^2 < 0$, (7) provides unbounded solutions. In that case, the system is said to be unstable. Finally, if $\xi_m^2 = 0$ for a certain perturbation, the problem reduces to a bifurcation case (analysed in Alcaraz *et al.*, 1997).

At the moment of the analysis, the stress components under the assumed biaxial loading are $\sigma_{11} = \sigma_1$ and $\sigma_{22} = \sigma_2$. Both components are supposed uniform in each material and σ_1 can be different, in general, in A and B.

It is convenient to express (5) in terms of the nominal stress rates $\dot{n}_{ij}$, which are related to Jaumann derivatives $\hat{\sigma}_{ij}$ and true stresses σ_{ij} by

$$\dot{n}_{11} = \dot{\sigma}_{11} - \sigma_1 \frac{\partial \dot{u}_1}{\partial x_1}$$

$$\dot{n}_{22} = \dot{\sigma}_{22} - \sigma_2 \frac{\partial \dot{u}_2}{\partial x_2}$$

$$\dot{n}_{12} = \dot{\sigma}_{12} - \frac{1}{2}(\sigma_1 + \sigma_2)\frac{\partial \dot{u}_1}{\partial x_2} + \frac{1}{2}(\sigma_1 - \sigma_2)\frac{\partial \dot{u}_2}{\partial x_1}$$

$$\dot{n}_{21} = \dot{\sigma}_{21} - \frac{1}{2}(\sigma_1 - \sigma_2)\frac{\partial \dot{u}_1}{\partial x_2} - \frac{1}{2}(\sigma_1 + \sigma_2)\frac{\partial \dot{u}_2}{\partial x_1}. \tag{11}$$

Using the constitutive eqns (5) and the incompressibility condition determined by $\dot{u}_{1,1} + \dot{u}_{2,2} = 0$, the linearization of (11) yields:

$$\bar{n}_{11} - \bar{n}_{22} = \left[2\mu^* - \frac{1}{2}(\sigma_1 + \sigma_2)\right]\left(\frac{\partial \bar{u}_1}{\partial x_1} - \frac{\partial \bar{u}_2}{\partial x_2}\right)$$

$$\bar{n}_{12} = \left[\mu + \frac{1}{2}(\sigma_1 - \sigma_2)\right]\frac{\partial \bar{u}_2}{\partial x_1} + \left[\mu - \frac{1}{2}(\sigma_1 + \sigma_2)\right]\frac{\partial \bar{u}_1}{\partial x_2}$$

$$\bar{n}_{21} = \left[\mu - \frac{1}{2}(\sigma_1 + \sigma_2)\right]\frac{\partial \bar{u}_2}{\partial x_1} + \left[\mu - \frac{1}{2}(\sigma_1 - \sigma_2)\right]\frac{\partial \bar{u}_1}{\partial x_2}. \tag{12}$$

If we now introduce a flow function $\psi(x_1, x_2)$ such that

$$\bar{u}_1 = \frac{\partial \psi}{\partial x_2}, \quad \bar{u}_2 = -\frac{\partial \psi}{\partial x_1} \tag{13}$$

and use (13) and (12) in (8) and (9), the following derivative equation can be derived:

$$(R+S)\frac{\partial^4 \psi}{\partial x_1^4} + 2(1-R)\frac{\partial^4 \psi}{\partial x_1^2 \partial x_2^2} + (R-S)\frac{\partial^4 \psi}{\partial x_2^4} + e^2\left(\frac{\partial^2 \psi}{\partial x_1^2} + \frac{\partial^2 \psi}{\partial x_2^2}\right) = 0 \tag{14}$$

where, to be concise, the following notation has been used:

$$R = \frac{\mu}{2\mu^*}, \quad S = \frac{\sigma_1 - \sigma_2}{4\mu^*}, \quad e^2 = \frac{\rho \xi^2}{2\mu^*} \tag{15}$$

and the corresponding continuity conditions at the interface are expressed by:

$$\left\langle \frac{\partial \psi}{\partial x_1} \right\rangle = \left\langle \frac{\partial \psi}{\partial x_2} \right\rangle = 0$$

$$\left\langle \left(4\mu^* - \mu - \frac{\sigma_1 + \sigma_2}{2}\right)\frac{\partial^3 \psi}{\partial x_1^2 \partial x_2} + \left(\mu - \frac{\sigma_1 - \sigma_2}{2}\right)\frac{\partial^3 \psi}{\partial x_2^3} + \rho \xi^2 \frac{\partial \psi}{\partial x_2} \right\rangle = 0$$

$$\left\langle -\left(\mu - \frac{\sigma_1 + \sigma_2}{2}\right)\frac{\partial^2 \psi}{\partial x_1^2} + \left(\mu - \frac{\sigma_1 - \sigma_2}{2}\right)\frac{\partial^2 \psi}{\partial x_2^2} \right\rangle = 0 \tag{16}$$

where the condition $\langle \bar{n}_{22} \rangle = 0$ is replaced by $\langle \bar{n}_{22,1} \rangle = 0$. On the other hand, the boundary conditions are also easily expressed in terms of the flow function ψ.

Equation (14) is said to be elliptic, hyperbolic or parabolic according to whether there are zero, four or two real roots, respectively, for its characteristic equation. As noted in

Alcaraz *et al.* (1997), real roots provide the characteristic planes of (14), allowing the possibility of strain discontinuity in the form of shear bands, and imaginary roots imply the existence of sinusoidal solutions around the interface. Here we are concerned with this last type of instability, the only mode encountered in the elliptic regime. The analysis that follows is centred on this regime, because it provides the most general solutions (complex conjugates) and, for this reason, could be considered to include the remaining regimes.

3. EIGENMODES. DEDUCTION OF THE GOVERNING EQUATION

We are now interested in finding the minimum eigenvalue ξ^2 corresponding to the first eigenmode (see (7) and (8)). As commented before, there will be stable or unstable conditions according to whether $\xi^2 > 0$ or $\xi^2 < 0$, respectively. It will be shown later that the magnitude ξ^2 also indicates the amount of instability in the process.

To determine the eigenmodes of the problem, let us seek for solutions of the flow function, ψ, in the form:

$$\psi = f(x_2)\sin\frac{2\pi x_1}{\lambda} \tag{17}$$

By inserting (17) into (14), the following differential equation for the function f is obtained:

$$(R-S)f^{IV} + [-2(1-R)\omega^2 + e^2]f'' + [(R+S)\omega^4 - e^2\omega^2]f = 0 \tag{18}$$

where $\omega = 2\pi/\lambda$.

As we are considering the elliptic regime, the roots of the characteristic equation of (18) are complex, and thus the resultant f functions that satisfy the boundary conditions $v_2(x_2 = a) = v_2(x_2 = c) = 0$ can be written as:

$$\begin{aligned} f_A &= \mathscr{R}\{c_1 \cdot \sin\omega\alpha(x_2 - a)\} \\ f_B &= \mathscr{R}\{c_2 \cdot \sin\omega\beta(c - x_2)\} \end{aligned} \tag{19}$$

where $\mathscr{R}$ denotes the real part of the enclosed quantity, and c_1 and c_2 are complex constants, and α and β, respectively, satisfy:

$$\begin{aligned} (R_A - S_A)\alpha^4 + [2(1-R_A) - b_A]\alpha^2 + [R_A + S_A - b_A] = 0 \\ (R_B - S_B)\beta^4 + [2(1-R_B) - b_B]\beta^2 + [R_B + S_B - b_B] = 0 \end{aligned} \tag{20}$$

where

$$q_A = \frac{2\pi}{\lambda}(b-a), \quad b_A = \frac{\rho_A\xi^2(b-a)^2}{2\mu^* q_A^2}, \quad q_B = \frac{2\pi}{\lambda}(c-b), \quad b_B = \frac{\rho_B\xi^2(c-b)^2}{2\mu^* q_B^2}.$$

Therefore,

$$\alpha^2 = \frac{R_A - 1 + b_A}{R_A - S_A} \pm i\sqrt{\frac{2R_A - 1 - S_A^2 - b_A^2}{R_A - S_A}}\sqrt{\frac{4 + b_A(1-R_A) - b_A(R_A - S_A)}{R_A - S_A}} \tag{21}$$

and an analogous expression for β^2.

The interface conditions (16) turn into:

$$\mathscr{R}\left\{c_1 \cdot \sin\frac{2\pi}{\lambda}\alpha(b-a)\right\} = \mathscr{R}\left\{c_2 \cdot \sin\frac{2\pi}{\lambda}\beta(c-b)\right\}$$

$$\mathscr{R}\left\{c_1 \cdot \alpha \cdot \cos\frac{2\pi}{\lambda}\alpha(b-a)\right\} = \mathscr{R}\left\{-c_2 \cdot \beta \cdot \cos\frac{2\pi}{\lambda}\beta(c-b)\right\}$$

$$\mathscr{R}\left\{c_1 \cdot [(R_A - S_A)\alpha^2 - (R_A + S'_A - 2 + b_A)]\alpha \cdot \cos\frac{2\pi}{\lambda}\alpha(b-a)\right\}$$

$$= \zeta\left[\mathscr{R}\left\{-c_2 \cdot [(R_B - S_B)\beta^2 - (R_B + S'_B - 2 + b_B)]\beta \cdot \cos\frac{2\pi}{\lambda}\beta(c-b)\right\}\right]$$

$$(R_A - S_A)\mathscr{R}\left\{c_1 \cdot \alpha^2 \cdot \sin\frac{2\pi}{\lambda}\alpha(b-a)\right\} - (R_A - S'_A)\mathscr{R}\left\{c_1 \cdot \sin\frac{2\pi}{\lambda}\alpha(b-a)\right\}$$

$$= \zeta(R_B - S_B)\mathscr{R}\left\{c_2 \cdot \beta^2 \cdot \sin\frac{2\pi}{\lambda}\beta(c-b)\right\} - (R_B - S'_B)\mathscr{R}\left\{c_2 \cdot \sin\frac{2\pi}{\lambda}\beta(c-b)\right\} \quad (22)$$

where

$$\zeta = \mu_B^*/\mu_A^*, \quad S' = \frac{\sigma_1 + \sigma_2}{4\mu^*}. \quad (23)$$

To facilitate the elimination of c_1 and c_2 in (22), several relations from (21) can be used:

$$\alpha^2(R_A - S_A) - (R_A + S'_A - 2 + b_A) = w_A + i\theta_A$$
$$(R_A - S'_A) - \alpha^2(R_A - S_A) = w_A - i\theta_A \quad (24)$$

where

$$w_A = 1 - S'_A - b_A/2$$
$$\theta_A = \sqrt{2R_A - 1 - S_A^2 - b_A^2/4 + b_A(1 - R_A) - b_A(R_A - S_A)} \quad (25)$$

and, by setting $\alpha = p_A + ir_A$

$$p_A^2 - r_A^2 = \mathscr{R}(\alpha^2) = \frac{R_A - 1 + b_A/2}{R_A - S_A}$$

$$p_A^2 + r_A^2 = |\alpha^2| = \sqrt{\frac{(R_A - S_A)(R_A + S_A - b)}{R_A - S_A}} = \sqrt{\frac{R_A + S_A - b}{R_A - S_A}} \equiv X_A \quad (26)$$

and similarly for $\beta = p_B + ir_B$.

After lengthy manipulations, (22) provides the following resultant equation:

$$(R_A - S_A)\left\{\frac{s_p^A}{p_A}[X_A(1 - S'_A - b_A/2) - S''_A + b_A/2]\right.$$
$$\left. + \frac{s_r^A}{r_A}[X_A(1 - S'_A - b_A/2) + S''_A - b_A/2]\right\}\left[\frac{s_p^B}{p_B} - \frac{s_r^B}{r_B}\right]$$
$$+ \zeta^2(R_B - S_B)\left\{\frac{s_p^B}{p_B}[X_B(1 - S'_B - b_B/2) - S''_B + b_B/2]\right.$$

$$+\frac{s_r^B}{r_B}[X_B(1-S'_B-b_B/2)+S''_B-b_B/2]\Big\}\left[\frac{s_p^A}{p_A}-\frac{s_r^A}{r_A}\right]$$

$$-\zeta\Big\{2(R_A-S_A)(R_B-S_B)[X_A(c_p^A+c_r^A)(c_r^B-c_p^B)+X_B(c_r^A-c_p^A)(c_r^B+c_p^B)]$$

$$+2(1-S'_A-b_A/2)(R_B-S_B)\left[\frac{s_p^A}{p_A}-\frac{s_r^A}{r_A}\right](p_Bs_p^B+r_Bs_r^B)$$

$$+(1-S'_A-b_A/2)(1-S'_B-b_B/2)\left[\frac{s_p^A}{p_A}-\frac{s_r^A}{r_A}\right]\left[\frac{s_p^B}{p_B}-\frac{s_r^B}{r_B}\right]$$

$$+4(R_A-S_A)(R_B-S_B)(p_As_p^A+r_As_r^A)(p_Bs_p^B+r_Bs_r^B)$$

$$+2(1-S'_B-b_B/2)(R_A-S_A)\left[\frac{s_p^B}{p_B}-\frac{s_r^B}{r_B}\right](p_As_p^A+r_As_r^A)\Big\}=0 \tag{27}$$

where

$$S''=\frac{RS'-(S^2+S'^2)/2}{R-S}$$

$$s_p=\sin 2pq \quad s_r=\sinh 2rq$$

$$c_p=\cos 2pq \quad c_r=\cosh 2rq. \tag{28}$$

4. GROWTH OF PERTURBATIONS. APPLICATION TO THE EXTRUSION PROCESS

Equation (27) relates the strain (ε), the wavenumber (q) and the stability parameter (ξ). Therefore, for a given strain ε, the set of eigenvalues, ξ, can be determined in terms of q.

When the minimum of these eigenvalues, ξ_m, satisfies the condition $\xi_m^2<0$, instability will occur and the displacement $\tilde{u}=e^{|\xi_m|t}\bar{u}$ (see (7)) will become an unbounded solution of the problem. Let $\tilde{u}_o$ be the initial amplitude of the perturbation. The evolution with time of the relative amplitude of the perturbation is then given by

$$\frac{\tilde{u}}{b-a}=e^{|\xi_m|t}\frac{\tilde{u}_o}{b-a}. \tag{29}$$

If this amplitude is limited by an allowable maximum, so that

$$\frac{\tilde{u}}{b-a}\leqslant M\frac{\tilde{u}_o}{b-a},$$

then

$$|\xi_m|\leqslant\frac{\ln M}{t}, \tag{30}$$

which provides a useful expression to control the maximum growth of the perturbation.

As an application of the above analysis, consider now the extrusion process of a bilayered sheet through a wedge-shaped die. Equation (27) can be used as a first approximation. It is assumed that the interface perturbation is initiated when the sheet contacts the entry section of the die. The growth of the perturbation is analysed according to actual values of the process.

Table 1. Constants in the constitutive models

Model	Constants	
Voce	$C = Y, m = 1$	$n = 12$
Hollomon	$k = Y$	$n = 0.04$
Prager	$C = Y$	$n = 7.3$

As shown later, instability is promoted as the maximum strain attained in the interface increases. In an extrusion process, this maximum occurs at the exit section of the die (see Alcaraz and Gil-Sevillano, 1993). Therefore, the perturbation amplitude under unstable conditions exhibits a maximum when the sheet leaves the die. Beyond this zone, as the material does not yield any longer, the perturbation will not increase any more.

The time required for the material to go through the die can be estimated from the following approximate expression:

$$t = \frac{\bar{\varepsilon}_{max}}{\dot{\bar{\varepsilon}}} \tag{31}$$

where $\bar{\varepsilon}_{max}$ represents the maximum strain of an interface element and $\dot{\bar{\varepsilon}}$ is the strain rate of the process. Then (30), turns into:

$$|\xi_m| \leqslant \frac{\dot{\bar{\varepsilon}} \ln M}{\bar{\varepsilon}_{max}}. \tag{32}$$

Considering a maximum strain of 1.0, a strain rate of 100 and a growth up to 20 times the initial small perturbation (i.e., $M = 20$), an allowable limit of 300 is obtained. This value can be used as a reference.

5. RESULTS

In this section, results are presented for materials with a constitutive equation in the form $\bar{\sigma} = \bar{\sigma}(\bar{\varepsilon})$, where $\bar{\sigma}$ and $\bar{\varepsilon}$ are the equivalent stress and strain, respectively. Three constitutive models have been considered in the calculations:

(i) Voce model: $\bar{\sigma} = C(1 - m\mathrm{e}^{-n\bar{\varepsilon}})$ (33)

(ii) Hollomon model: $\bar{\sigma} = k\bar{\varepsilon}^n$ (34)

(iii) Prager model: $\bar{\sigma} = C\tanh(n\bar{\varepsilon})$ (35)

where C, k, m, n are constants. Details of the choice of values for these constants are given in Alcaraz *et al.* (1997). The relevant information is summarized in Tables 1 and 2.

Table 2. Parameters in the governing equation (27) for the constitutive models

Voce	$R = \sqrt{\frac{3}{2}}\frac{1}{2n}\left(\frac{\mathrm{e}^{n\bar{\varepsilon}}}{m} - 1\right)\coth\left(\sqrt{\frac{3}{2}}\bar{\varepsilon}\right)$	$S = \sqrt{\frac{3}{2}}\frac{1}{2n}\left(\frac{\mathrm{e}^{n\bar{\varepsilon}}}{m} - 1\right)$
$\bar{\sigma} = C(1 - m\mathrm{e}^{-n\bar{\varepsilon}})$	$S' = \frac{3}{2}\frac{\sigma_B}{Cmn\mathrm{e}^{-n\bar{\varepsilon}}}$	$\zeta = \frac{C_B m_B n_B}{C_A m_A n_A}\mathrm{e}^{(n_B - n_A)\bar{\varepsilon}}$
Hollomon	$R = \sqrt{\frac{3}{2}}\frac{\bar{\varepsilon}}{n}\coth\left(\sqrt{\frac{3}{2}}\bar{\varepsilon}\right)$	$S = \sqrt{\frac{3}{2}}\frac{\bar{\varepsilon}}{n}$
$\bar{\sigma} = k\bar{\varepsilon}^n$	$S' = \frac{3}{2}\frac{\sigma_B}{kn\bar{\varepsilon}^{n-1}}$	$\zeta = k_r\frac{n_B}{n_A}\bar{\varepsilon}^{n_B - n_A}$
Prager	$R = \sqrt{\frac{3}{2}}\frac{1}{2n}\sinh(2n\bar{\varepsilon})\coth\left(\sqrt{\frac{3}{2}}\bar{\varepsilon}\right)$	$S = \sqrt{\frac{3}{2}}\frac{1}{2n}\sinh(2n\bar{\varepsilon})$
$\bar{\sigma} = C\tanh(n\bar{\varepsilon})$	$S' = \frac{3}{2}\frac{\sigma_B}{Cn}\cosh^2(n\bar{\varepsilon})$	$\zeta = \frac{C_B n_B}{C_A n_A}\frac{\cosh^2(n_A\bar{\varepsilon})}{\cosh^2(n_B\bar{\varepsilon})}$

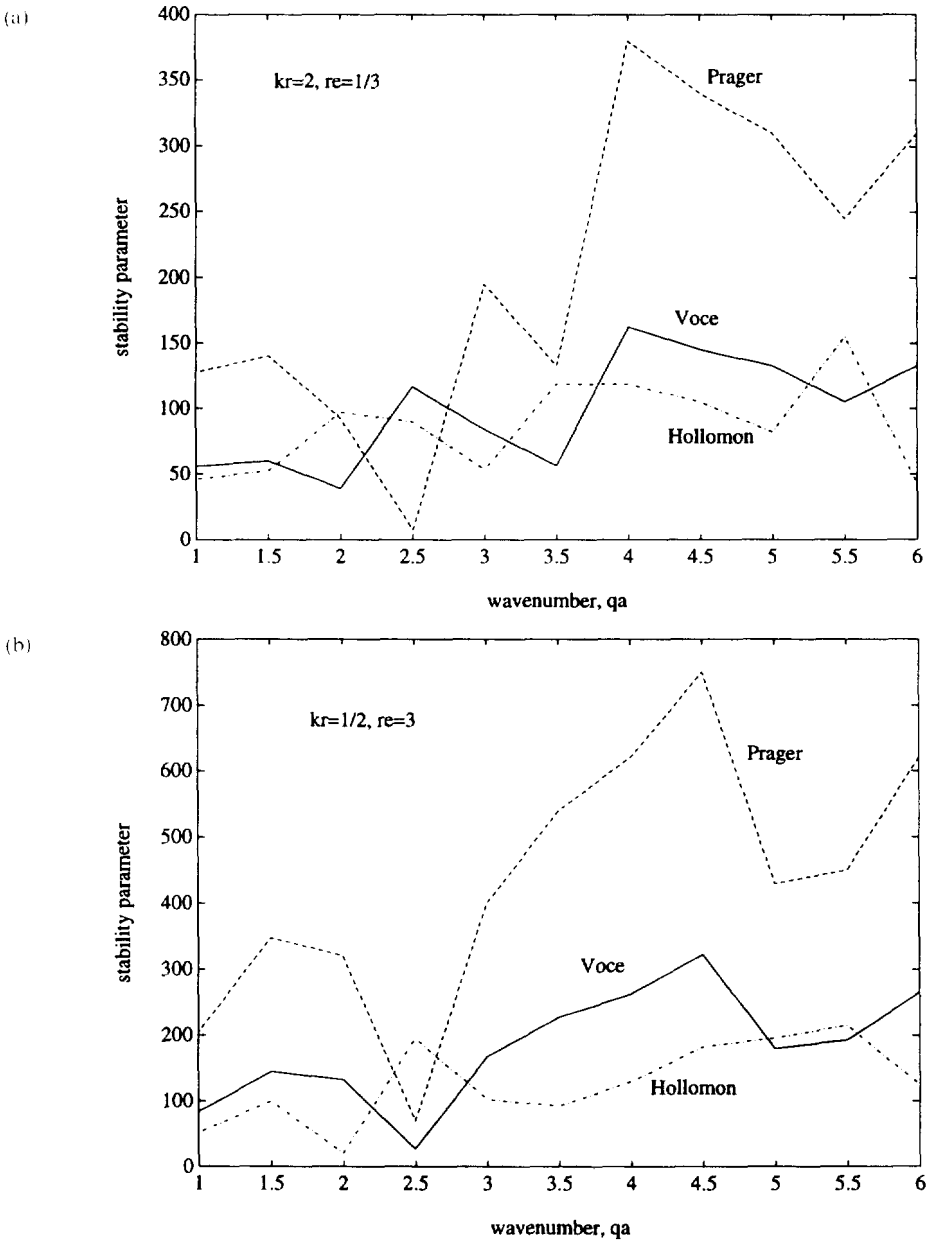

Fig. 2. Influence of the constitutive model on the stability parameter ξ: (a) $kr = Y_2/Y_1 = 2$, $re = e_2/e_1 = 1.3$, (b) $kr = Y_2/Y_1 = 1.2$, $re = e_2/e_1 = 3$.

Table 1 shows the selected values of the parameters in the constitutive laws, and Table 2 gives the expressions for R, S, S' and ζ corresponding to each constitutive equation.

5.1. *Influence of the constitutive models*

Firstly, the effect of the selected constitutive model on instability is assessed. Figure 2 shows the results for the three constitutive models, in two typical cases: (a) a bilayer with an upper location of the harder material, a yield stress ratio $k_r = Y_B/Y_A = 2$ and a thickness ratio $r_t = (c-b)/(b-a) = 1.3$ (in Fig. 2a), and (b) a bilayer with a lower location of the harder material with ratios $k_r = 1/2$ and $r_t = 3$ (in Fig. 2b). The harder material could be a corrosion resistant alloy and the other a low-alloyed structural steel. In all the cases, a maximum strain of 1.0 is assumed.

It can be seen that the values of the stability parameter, ξ, using the Prager equation are higher than those obtained with the Voce model, and the latter, in turn, higher than those corresponding to the Hollomon model. Therefore, the Hollomon equation leads to a

Table 3. Reference values for both locations of the harder material

Location of the harder material	k_r	r_c	n_a	n_b	p_r^a	p_r^b	$d_a\ d_b$	ε_{max}
Upper	2	1.3	12	12	1	1	1	1
Lower	0.5	3	12	12	1	1	1	1

more stable behaviour. However, the Voce or Prager equations are more representative of an actual high-temperature plastic behaviour, by which a saturation stress is often reached after only moderate strains.

Comparing now the results of Fig. 2a and Fig. 2b, it is clearly seen that for a lower location of the harder material (Fig. 2b), a higher stability parameter is obtained. By assuming the reference value of 300, it is concluded that this limit is exceeded in both cases by using the Prager model, especially when the harder material is placed lower.

5.2. *Influence of the geometric and material parameters of the problem*

A number of calculations have been carried out in order to ascertain the influence of several geometric and material variables on the stability parameter. The computations have been performed using the Voce model. In particular, the following variables are considered:

- the yield stress ratio, $k_r = Y_B/Y_A$ (for both locations of the harder layer),
- the thickness ratio, $r_c = (c-b)/(b-a)$ (also for both locations),
- the hardening parameters n_a and n_b,
- the hydrostatic stress parameter, $p_r = \sigma_h/Y$, where σ_h is the hydrostatic stress,
- the density ratio d_a/d_b,
- the maximum strain.

The reference values of the parameters for both locations of the harder materials are given in Table 3.

Figure 3 shows the effect of the yield stress ratio, k_r, for both locations of the harder material. Note that these graphs start at the wavenumber corresponding to the onset of the elliptic regime, since we focus on the undulatory mode at the interface. This criterion will be followed in the subsequent results of this section. In Fig. 3, it can be seen that the *maximum* stability parameter increases as the discrepancy between the yield stresses of the two materials increases. Values are again higher in the case of setting lower the harder material (Fig. 3b). In this latter case, the limit of 300 is only reached for a wavenumber of 4.5 if $k_r < 0.5$, and for a wavenumber of 6 if $k_r < 0.33$.

Therefore, putting together the results of Alcaraz *et al.* (1997) and the present results, it can be drawn that the discrepancy in the yield stress not only promotes the onset of instabilities but also the subsequent growth of the undulations originated at the interface.

Figure 4 illustrates the influence of the thickness ratio, r_c. No trend can be appreciated in this case. Nevertheless, Fig. 4a, for an upper location of the harder layer, seems to indicate a slight increase in the maximum stability parameter with the increase in the thickness of the harder layer. The stability parameter is higher in Fig. 4b, corresponding to the lower location of the harder material. In this last case, the reference value of 300 is attained at certain wavenumbers.

Figure 5 shows the effect of some other parameters, for the case of a lower harder material, which proves to be the most dangerous. The effect of the hydrostatic stress in material A is shown in Fig. 5a. The results indicate a slight increasing trend on increasing the hydrostatic stress. It is also found that the wavenumber of 4.5 appears to provide the worst conditions for stability.

Figures 5b and c illustrate the influence on stability of the hardening parameters n_a and n_b, respectively. It can be seen that ξ considerably increases as either of the hardening parameters increases. A hardening coefficient n_b higher than 12 provides stability parameters exceeding the reference limit of 300 at high wavenumbers.

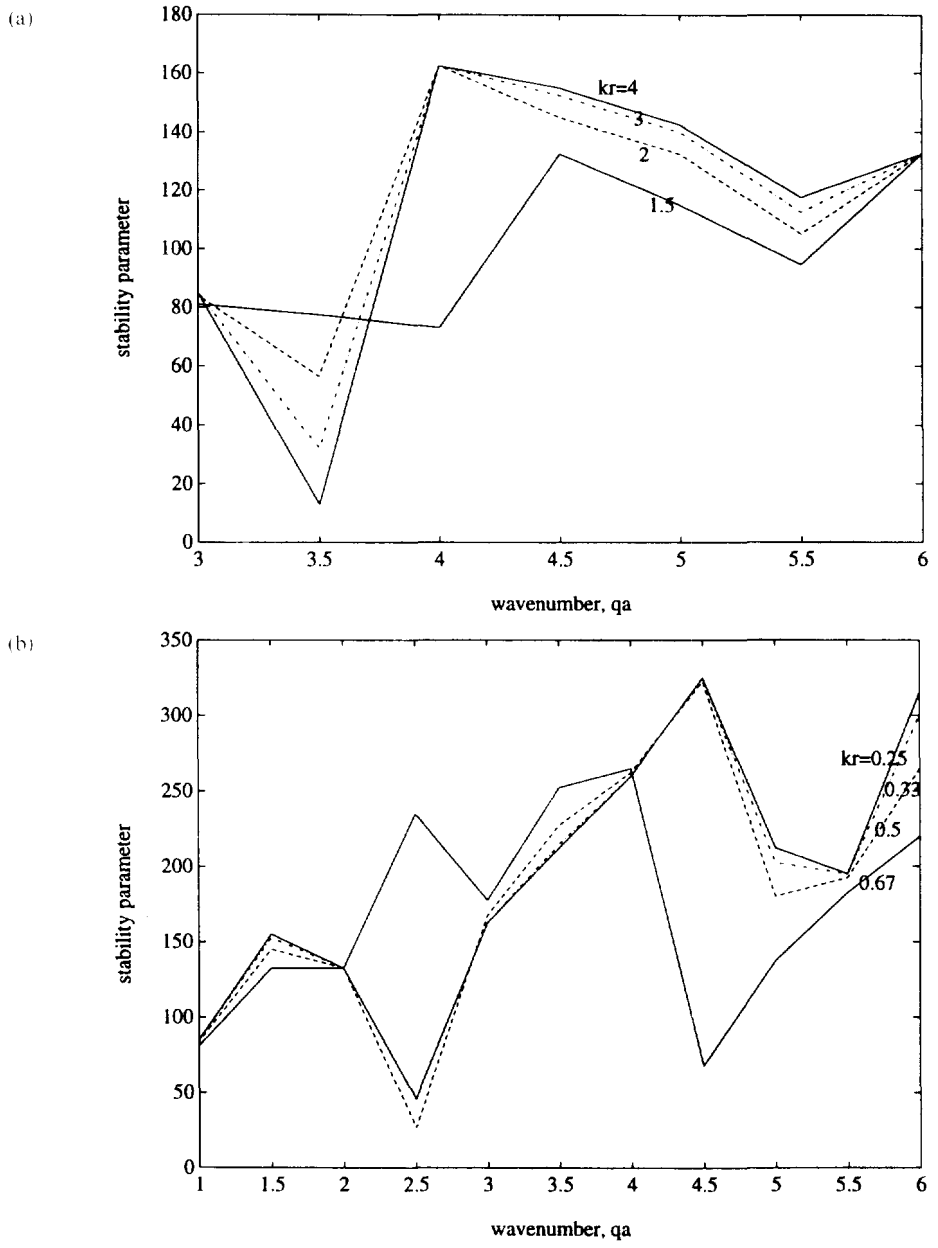

Fig. 3. Influence of the yield stress ratio, k_r, on the stability parameter ξ: (a) upper harder material, (b) lower harder material.

Consequently, as occurred with the yield stress ratio, a similar trend in the hardening and hydrostatic pressure parameters has been found between the present analysis and the bifurcation analysis.

The density ratio also has repercussions on the bifurcation equation, due to the dynamic nature of the stability phenomenon. From Fig. 5d, it appears that the growth of the perturbation very slightly increases as it does the lower/upper density ratio.

The effect on ξ on the maximum strain attained at the interface, shown in Fig. 5e, becomes more relevant. An increase in the strain provides a very marked increase in ξ values. In the extrusion process, for instance, this situation would be produced by an increase in the die angle or in the extrusion ratio. Consequently, as indicated by the high values attained in Fig. 5e, instability problems may be encountered at high strains for perturbations developed along the bimaterial interface.

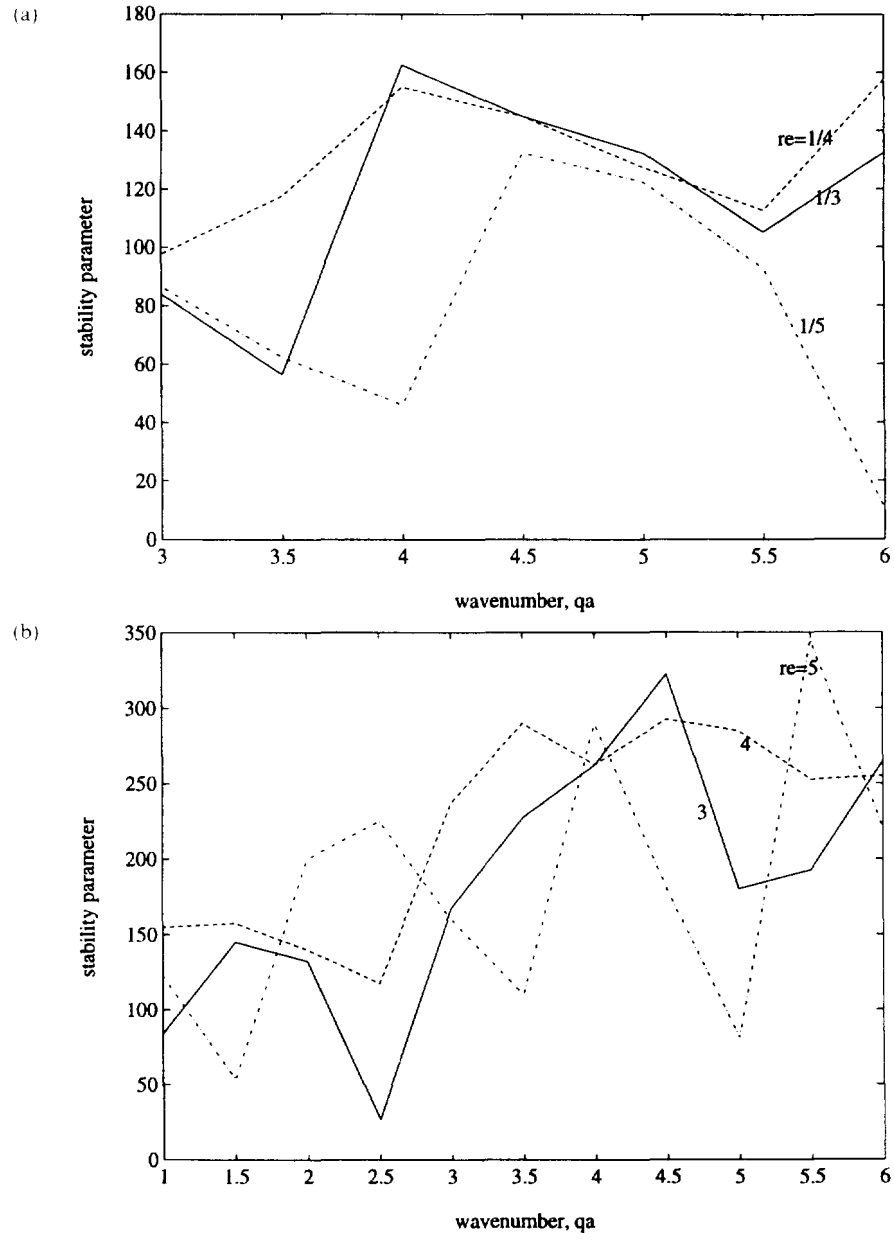

Fig. 4. Influence of the thickness ratio, r_e, on the stability parameter ξ: (a) upper harder material, (b) lower harder material.

6. CONCLUSIONS

The analysis carried out in this paper completes the bifurcation analysis of bimetallic layers between rigid surfaces under biaxial plastic loading, presented in Alcaraz *et al.* (1997). A stability parameter is established to determine the growth of an initial perturbation originated at the interface, in terms of the strain rate, the total plastic strain and the other geometric and material parameters of the process. Detailed results are presented about the effect of a number of variables related to the problem, such as the yield stress ratio, the thickness ratio, the hardening parameters, the maximum strain attained and the hydrostatic stress.

In summary, it can be concluded that instability is originated and promoted as the yield stress ratio between the harder and softer material increases. The same, yet stronger, tendency is found on increasing the maximum strain attained at the interface or the hardening parameters of the constitutive laws. The density ratio between the two materials and the hydrostatic stress levels affects weakly the stability of the process: an increase in

(a)

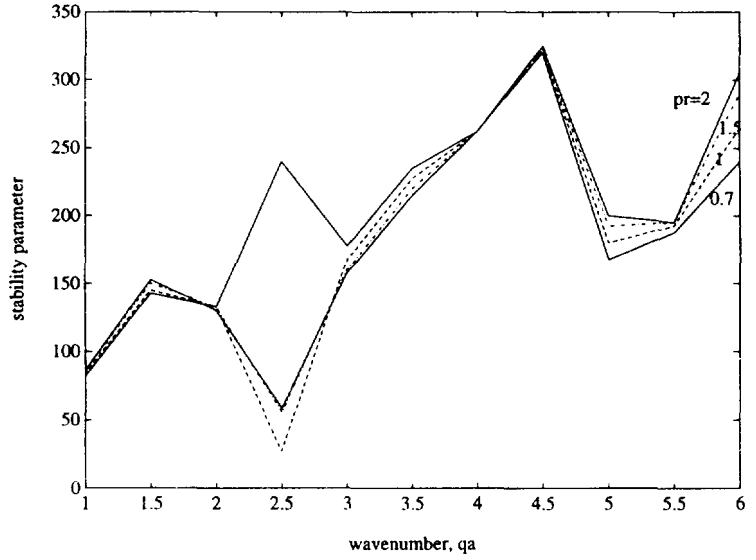

(b)

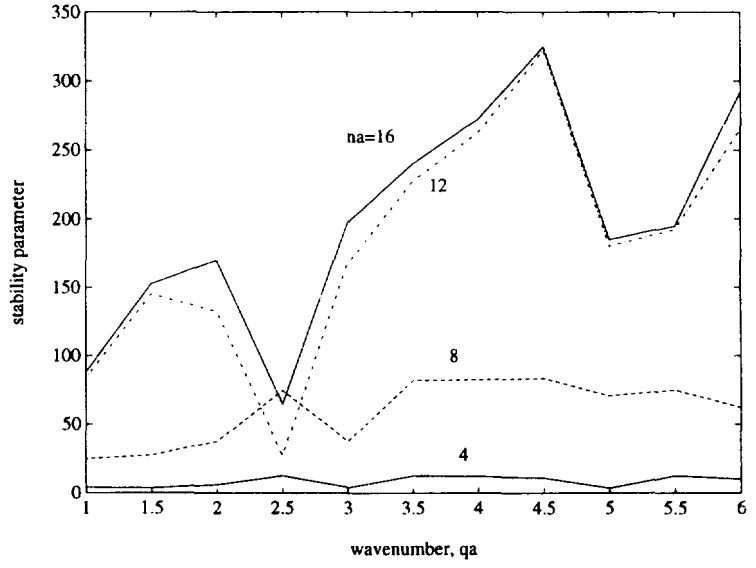

(c)

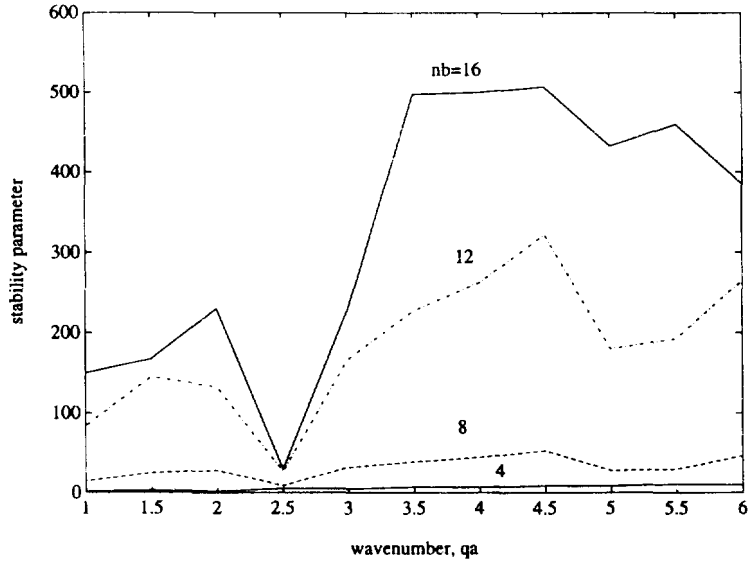

Fig. 5. Effect on the stability parameter ξ, for a lower location of the harder component, of: (a) the hydrostatic stress, $p_* = \sigma_{ii}/Y_{ave}$, in A, (b) the hardening parameter n_a, (c) the hardening parameter n_b, (d) the density ratio $dr = d_b/d_a$, (e) the maximum strain, m.s., at the bimaterial interface.
(*Continued overleaf.*)

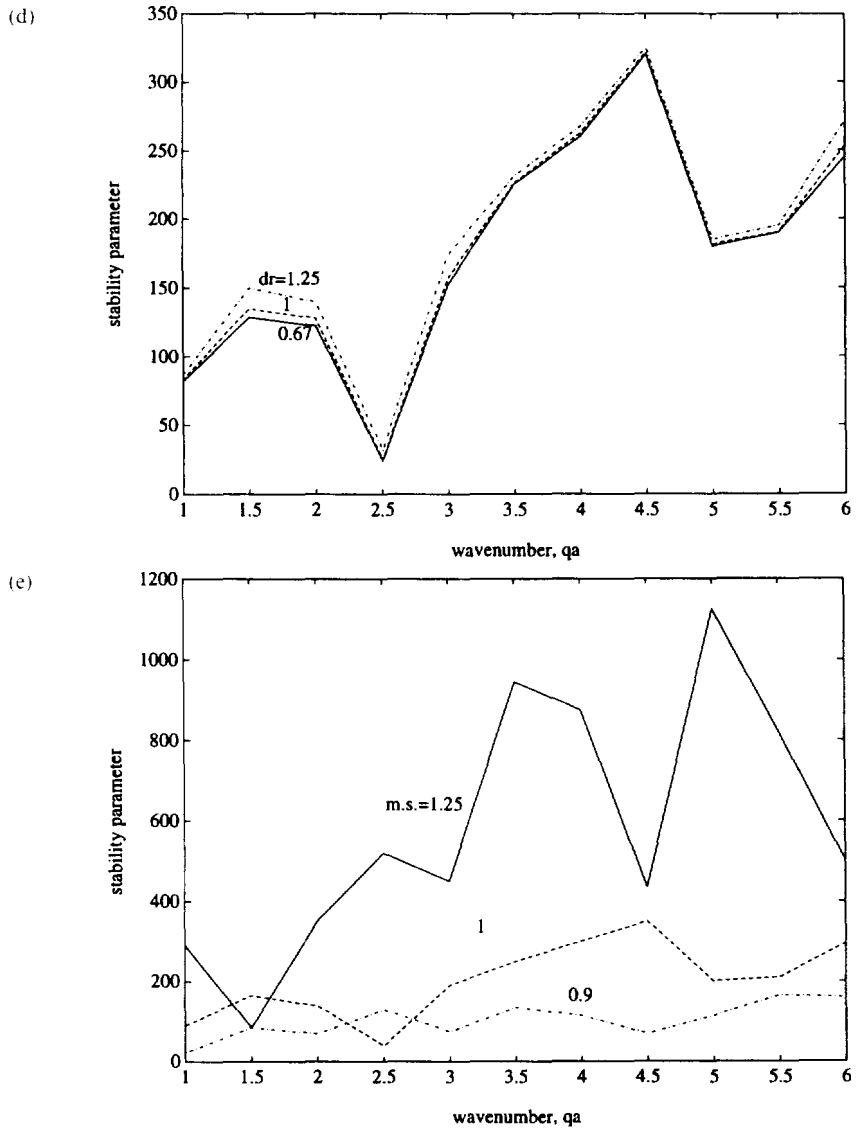

Fig. 5. (*Continued*).

the lower/upper density ratio, or in the hydrostatic stress level, promotes the growth of instabilities.

It is also shown that instability is generally favoured with a lower location of the harder material. The values of the stability parameters are almost doubled compared with the opposite case.

Finally, the influence of the selected constitutive model is illustrated. Among the three models considered (Voce, Prager and Hollomon), the Prager model appears to provide the worst conditions for stability.

REFERENCES

Alcaraz, J. L. and Gil-Sevillano, J. (1993). Optimizing the production of sound bimetallic tubes by using ABAQUS. In *Proc. ABAQUS Users' Conference*, 23–25 June, Aachen, Germany, pp. 39–53.

Alcaraz, J. L., Martínez-Esnaola, J. M. and Gil-Sevillano, J. (1997). Interface stability under biaxial loading of bilayered sheets between rigid surfaces—I. Bifurcation analysis. *Int. J. Solids Struct.* **34**, 603–623.

Biot, M. A. (1965). *Mechanics of Incremental Deformation*. Wiley, New York.

Dudzinski, D. and Molinari, A. (1991). Perturbation analysis of thermoviscoplastic instabilities in biaxial loading. *Int. J. Solids Struct.* **27**, 601–628.

Hill, R. and Hutchinson, J. W. (1975). Bifurcation phenomena in the plane tension test. *J. Mech. Phys. Solids* **23**, 239–264.

Triantafyllidis, N. and Lehner, F. K. (1993). Interfacial instability of density-stratified two-layer systems under initial stress. *J. Mech. Phys. Solids* **41**, 117–142.